Progress In Electromagnetics Research Letters, Vol. 56, 115–122, 2015

Transmission Line Theory and Thermal Analysis of Coaxial Coupler for TWTs

Rupasree Roy[1, *], Vishant Gahlaut[1], Abhishek Jain[2], Parvez A. Alvi[1], Sanjay K. Ghosh[2], and Ashok K. Sinha[2]

Abstract—This paper presents the transmission line analysis, thermal and structural analysis of a multi-section coaxial coupler (MSCC) used in traveling-wave tubes (TWTs) to handle high average power over a wide frequency range. Power transmission through coupler from the device demands very good matching between load and source impedances such that low voltage standing wave ratio (VSWR) is achieved. Modeling of the MSCC for wideband TWTs in commercially software packages takes very long iteration time even in high-end computers. An analytical approach has been developed to model MSCC which takes less iteration time even in ordinary computer. Analytical results have been compared to those obtained from CST microwave studio. Finally, thermal and structural analysis has been carried out to study the thermal aspects for handling high average RF power.

1. INTRODUCTION

Coaxial couplers are used in traveling-wave tubes (TWTs) to feed and extract RF power into and from interaction structure/slow wave structure (SWS) respectively [1–5]. However, output coupler has to handle medium to high average power, hence, there must be minimum reflection of RF power so that heat load may also be minimized. Coaxial couplers are suitably modeled to achieve better return loss and voltage standing wave ratio (VSWR) or to minimize reflection of RF signals, by transforming frequency dependent characteristic impedance (Z_0) of helix [6] to standard connectors (Z_L). For transformation of source impedance (Z_0) to load (Z_L), coaxial line is broken into quarter wave and further sub-quarter wave transformers through proper impedance matching, so that reflection from individual transformer is minimized. For modeling or analysis of MSCC [7–9], different commercially available software packages, namely, CST microwave studio [10] and HFSS [11], take very long time and use fixed Z_L. But, Z_L varies from connector to connector due to fabrication tolerances, and it affects S-parameters of the coupler. To analyze MSCC, an analytical model, based on reflection approach [8], has been developed to predict S-parameters by transforming frequency dependent Z_0 to Z_L and also by minimizing reflections from each quarter wave transformer, and results can be obtained in few minutes.

For proper transformation of Z_0 to Z_L, the center conductor of the coupler is broken into quarter-wave to sub-quarter wave transformer, hence so called MSCC. For high gain TWTs ($> 55\,\text{dB}$), reflection of RF signal must be minimized from each transformer so that adequate VSWR or S-parameters are obtained. Reflection of RF signal causes back-and-fourth oscillation in the TWT, generates heat at the helix to coupler joint and finally leads the TWT into destruction.

MSCC, realized with center conductor — comparable to wavelength, outer conductor, window ceramic disk, etc., (Figure 1), has to incorporate high vacuum inside the TWT and also has to handle medium to high average RF power. However, conductor loss (ohmic loss) of center conductor, in addition to dielectric loss, restricts average power handling capability of coupler. Under hot condition (during

Received 16 August 2014, Accepted 27 October 2014, Scheduled 30 September 2015

* Corresponding author: Rupasree Roy (ghoshrg71@rediffmail.com).
[1] Department of Physics, Banasthali University, Banasthali, Rajasthan 304022, India. [2] Microwave Tubes Division, Central Electronics Engineering Research Institute (Council of Scientific and Industrial Research (CSIR)), Pilani, Rajasthan 333031, India.

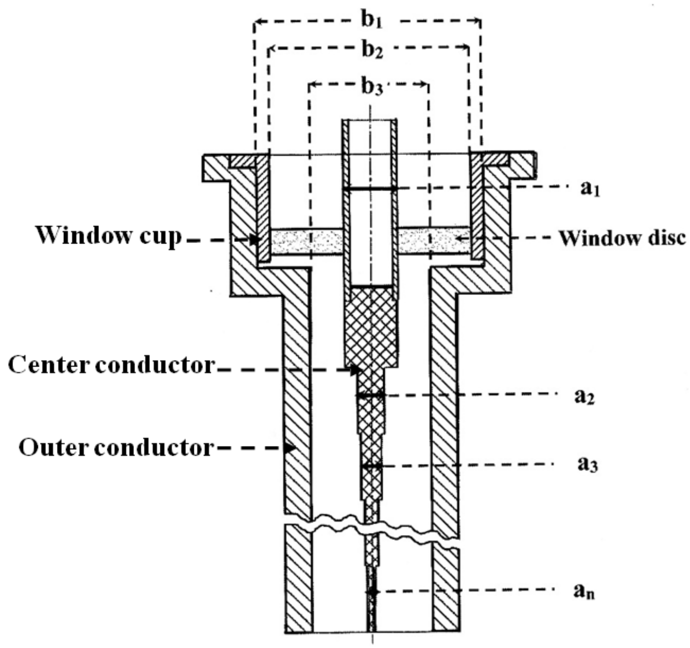

Figure 1. Schematic view of the multi-section coaxial coupler.

extraction of high power), thermal load, structural deformation, stresses at different braze joints are important key parameters to study. Fabrication tolerances of coupler components enhance impedance mismatch causing power loss in the coupler which in turn increases thermal load. The increase in thermal load acts on thermal expansion, deformation of constituent components and also enhances stress at different braze joints, which finally add to the impedance mismatch. Hence, thermal and structural analyses of coaxial coupler are also important [4].

In this paper the authors present transmission line analysis and thermal analysis of a wideband coaxial coupler for high average power ($\sim$200 W) application. The dimensions of the constituent elements of coaxial coupler have been modeled analytically and then verified with CST. Here, it is shown that if dimensions (b/a) of any transformer are deviated from the optimized value, reflection (Γ) from each transformer is affected and finally VSWR. Thus, this model helps to optimize coaxial couplers for any application over any desired frequency range by optimizing dimensions of each transformer. This model includes effect of window disc material properties, dimensions, in addition to generalized 'n' number of transformers and also takes less iteration cycle in ordinary computer. Thermal and structural analysis helps to decide power handling capability of the coupler and thermal management issues of the window disc.

2. ANALYSIS

To analyze the MSCC, reflection approach has been used to predict reflections from each section of the quarter wave transformer and has been optimized by varying b/a of each transformer ('b' is the inner radius of the outer conductor and 'a' the outer radius of the inner conductor) by proper impedance matching of successive transformer. For proper matching of the MSCC with the helix, it has been broken into quarter-wave transformer which is further broken into sub-quarter wave transformer so that minimum reflection occurs (Figure 2). Thus, the reflection coefficient of Nth section can be given as [8]:

$$\sum_{p=0}^{N} \Gamma_p = \frac{Z_{p+1} - Z_p}{Z_{p+1} + Z_p}, \quad p = 1, 2, 3, \ldots, N. \tag{1}$$

with Z_1 (for $p = 1$) is the impedances of the first electrical sections of length $\theta_1 = \beta l_1$ and for $p = N$, $Z_{N+1} = Z_L$. Z_L is the load impedance equals to the impedances of the Nth electrical sections of length

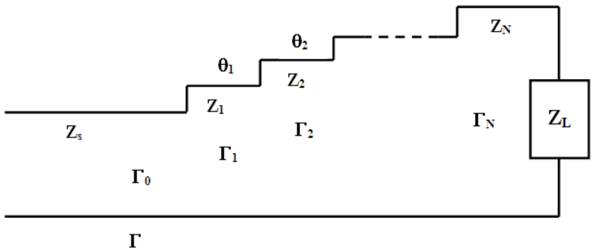

Figure 2. Analytical model of MSCC — multi-section sub-quarter wave model.

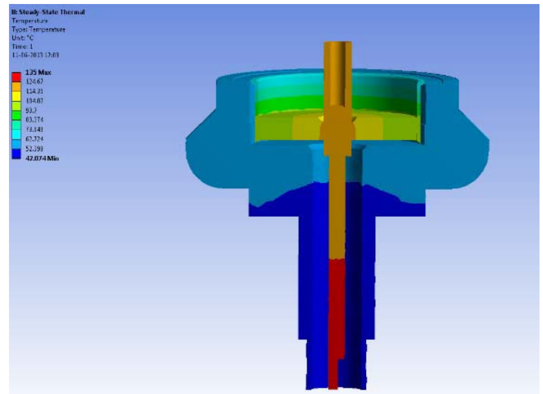

Figure 3. Temperature distribution at different regions of MSCC.

Table 1. Necessary and input boundary condition.

Heat Power	At window 1.4 W
temperature	135°C at output helix tape
Ambient temp.	25°C
Radiation	At all open surfaces with emissivity according to material.

Table 2. Necessary and input boundary condition.

Interface	**TCC (W/m^2K)**
Center pin-helix tape	25,000
Helix tape-APBN support rod	10,000
APBN support rod-IPP barrel	25,000
Barrel-base plate	25,000

$\theta_N = \beta l_N$ with l the physical length of the transformer and β $(= 2\pi/\lambda)$ propagation constant.

Thus, from (1), the reflection coefficient of the last section can be given as:

$$\Gamma_N = \frac{Z_L - Z_N}{Z_L + Z_N} \tag{2}$$

Hence, using (1) and (2), the total reflection coefficient, the sum of the first-order reflected waves only, can be given as [8]:

$$\begin{aligned}\Gamma &= \Gamma_0 + \Gamma_1 \exp(-2j\theta_1) + \Gamma_2 \exp\{-2j(\theta_1+\theta_2)\} + \Gamma_3 \exp\{-2j(\theta_1+\theta_2+\theta_3)\} \\ &\quad + \ldots + \Gamma_N \exp\{-2j(\theta_1+\theta_2+\ldots+\theta_N)\}\end{aligned} \tag{3}$$

$$VSWR = \frac{1+|\Gamma|}{1-|\Gamma|} \tag{4}$$

$$RL = \frac{VSWR-1}{VSWR+1}\,\text{dB} \tag{5}$$

Thus, total reflection coefficient from the MSCC can be predicted using Equation (3), and hence, the return loss/VSWR can be obtained for any coaxial coupler over any frequency range using (4)–(5).

Using the analytical Expressions (1) to (5), a computer code has been developed in MATLAB to predict the S parameters, namely VSWR and return loss (RL). Attempts have been made to generalize the programme to consider 1) frequency dependent helix characteristic impedance for any structure, 2) variation of connector impedance, 3) 'n' numbers of transformers, and 4) shape, size and material property of the window disc.

3. THERMAL ANALYSIS

In the thermal model (Figure 3), input boundary conditions are the heat load, and thermal conductance are given in Tables 1 and 2, respectively. Heat load on the ceramic window is the power loss — sum of power loss due to mismatch of impedance, conductor loss, dielectric loss, etc. Also, another thermal source of the coupler is the conducted heat from the helical structure, arising due to helix interception current. In the present study, helix temperature is ∼135°C arising due to 2 mA interception current operating at 6 kV, obtained from thermal analysis in ANSYS. Temperature distributions at different structure regions, structural deformation and stress at different joints have been studied.

4. RESULTS AND DISCUSSION

Transmission line analysis and thermal analysis of a MSCC (Figures 1–3) has been carried out for wideband application. To validate the analytical results structure dimensions are chosen from an existing Ku band TWT. Analytical results have been validated with CST Microwave Studio, and finally thermal and structural analysis have been carried out for structural integrity due to medium to high power propagation.

The characteristic impedance of the helix SWS (Z_0) has wide range of variation over the frequency (Figure 4) and needs to be transformed to the standard connector impedance (Z_L) to achieve proper matching of impedances which is quantified in terms of S parameters or VSWR. Thus, to make a tradeoff between high impedance at lower frequency and low impedance at high frequency, optimization of b/a for each transformer is very important and needs several iteration. Moreover, due to high power (∼200 W CW) propagation heat load of the coupler deforms cold structure dimensions of the constituent elements which demands for thermal and structural analysis before optimizing cold b/a of transformers.

Based on the analytical model (Figure 2), a MSCC of five transformers have been suitably modeled optimizing b_n/a_n ratio ($n = 1, 2, \ldots, 5$) to get suitable VSWR (Figure 5). Optimized dimensions for Ku-band space TWT under development at CEERI are as follows: $b_1/a_1 = 6.37$, $b_2/a_2 = 6.17$, $b_3/a_3 = 1.96$, $b_4/a_4 = 4.0$, $b_5/a_5 = 6.66$ with $b_1 = 6.3$, $b_2 = 6.5$, $b_3 = b_4 = b_5 = 2.0$ and solid line in Figure 5 represents corresponding VSWR. By changing 'a' or b/a of any section, here it is $b_1/a_1 = 3.1$, VSWR of the coupler changes and represented by broken line in Figure 5. It is more important to say that by changing b_1/a_1 as depicted in Figure 5, reflection from individual transformer also varies (Figure 6), and this is due to mismatch of impedances of transformers. Reflections from each transformer are represented by Γ_1 (load end) to Γ_5 (source end) in Figures 6(a) to 6(e), respectively. Solid line in these figures represents reflection corresponding to optimized dimensions and broken line corresponding to change in b_1/a_1 depicted in Figure 5. Any change of b_n/a_n corresponding to any transformer affects reflection from individual transformer and finally VSWR of the coupler. Thus to minimize reflection from individual sections and to get suitable VSWR, one needs several iterations to optimize dimensions, and this analytical model takes significantly less time than commercial software packages. Standard connectors also have great impact on S-parameter for a given Z_0 and optimized b/a ratios (Figure 7).

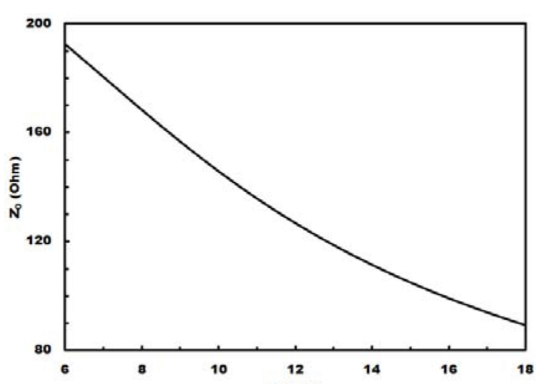

Figure 4. Variation of characteristic impedance (Z_0) of helix with frequency (mean helix radius = 0.755 mm, mean to outer helix radius = 1.1, mean helix to envelope radius = 2.4, tape width to pitch = 0.5).

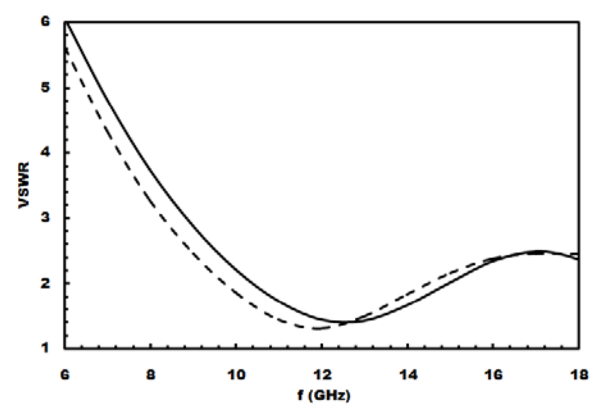

Figure 5. VSWR of the coaxial coupler: (Solid line: $b_1/a_1 = 6.37$, $b_2/a_2 = 6.17$, $b_3/a_3 = 1.96$, $b_4/a_4 = 4.0$, $b_5/a_5 = 6.66$ with $b_1 = 6.3$, $b_2 = 6.5$, $b_3 = b_4 = b_5 = 2.0$. Broken line is for $b_1/a_1 = 3.1$, remaining dimensions constant.

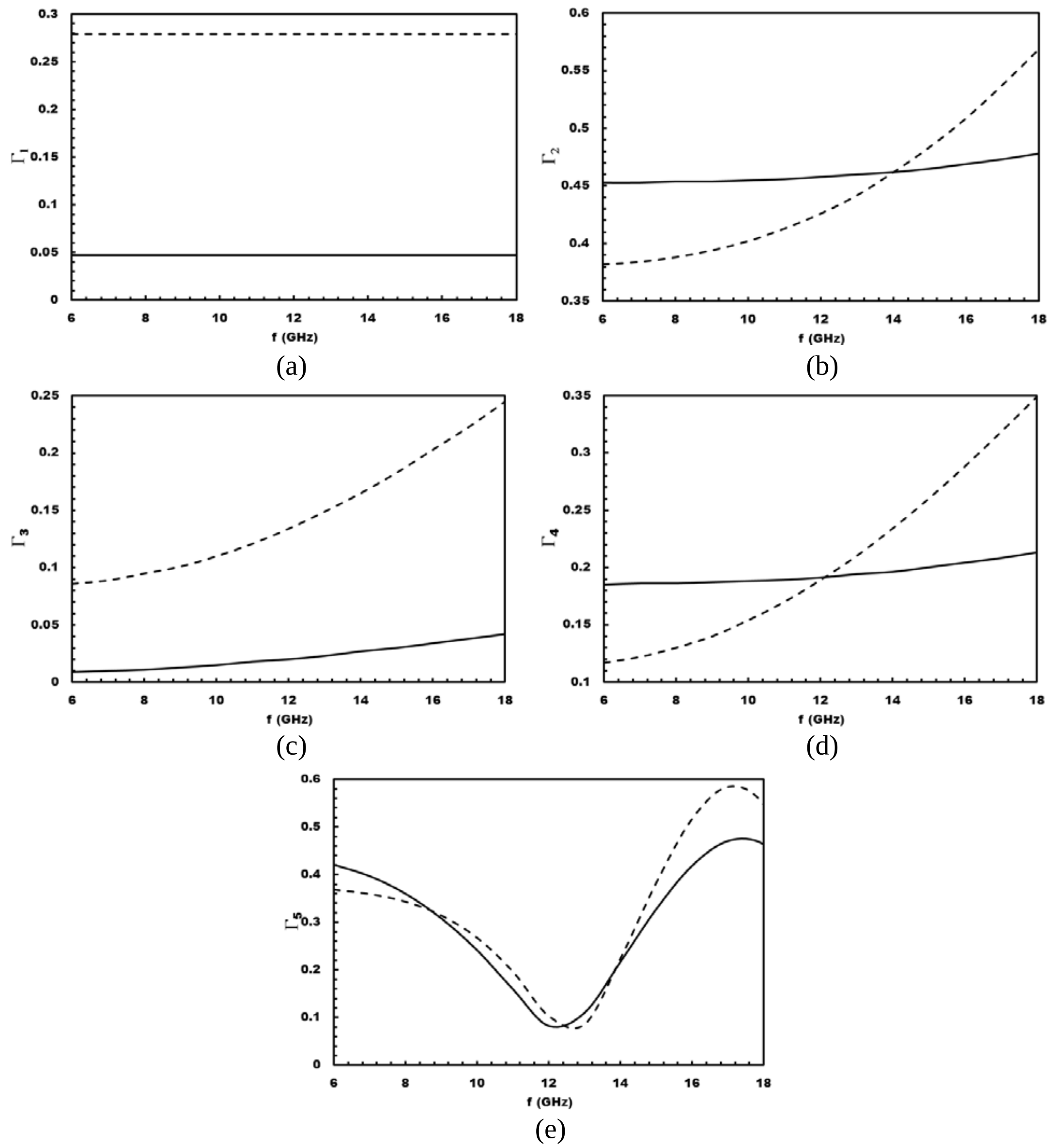

Figure 6. Reflection from (a) first section (Γ_1), (b) second section (Γ_2), (c) third section (Γ_3), (d) fourth section (Γ_4) and (e) fifth section (Γ_5) (solid and broken line dimensions are given in Figure 5).

It can be seen from Figure 7 that with the variation of connector, VSWR varies. This is because the variation of impedance (Z_L) mismatch of transformers occurs. Hence, one may need to optimize b_n/a_n such that impedance of the first section agrees with connector impedance.

The window disc material plays several rolls in designing MSCC for TWTs, namely, optimization of S-parameter, to incorporate vacuum, thermal management, etc. Dimension and material property (permittivity) of the window disc affect VSWR of the coupler (Figure 8). Here, study has been done for two window disc materials, namely, alumina ($\varepsilon_r = 9.0$) and CVD diamond ($\varepsilon_r = 5.6$). From the Figure 8, it can be seen that with the variation of permittivity of the window disc, keeping thickness (0.9 mm) and diameter (6.3 mm) constant, VSWR improves with increase in permittivity (alumina) at lower frequency, and the effect is reverse at higher frequency. Thus there is a tradeoff in selecting window disc material, but aluminum is a suitable choice for cost effectiveness and analytical results with alumina window disc have also been verified with CST microwave studio (Figure 9). It can be seen (Figure 9) that the two results agree closely. It can be seen from Figure 9 that there is a dip at

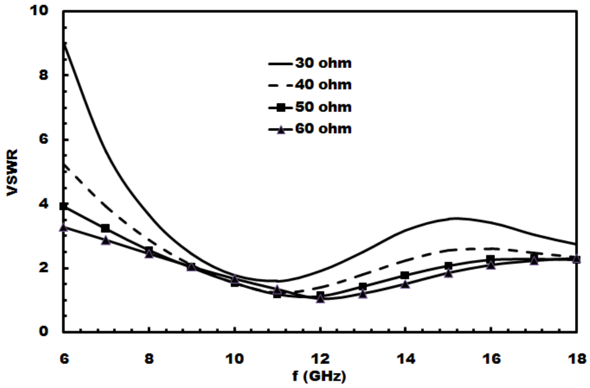

Figure 7. Effect of connector (Z_L) on VSWR (dimensions are depicted in Figure 5 corresponding to solid line).

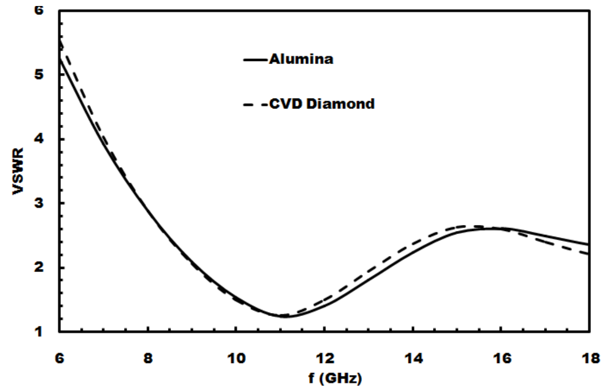

Figure 8. Effect of permittivity (ε_r) of window disc material on VSWR (dimensions are depicted in Figure 5 corresponding to solid line).

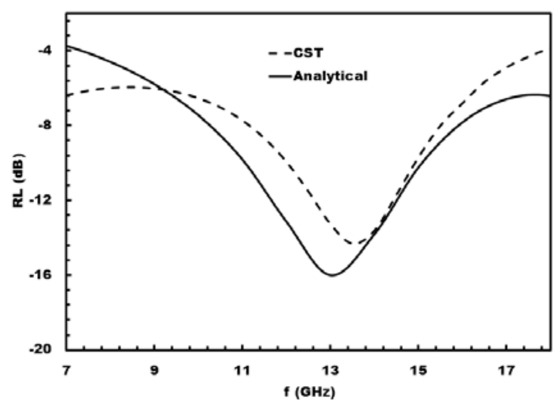

Figure 9. Comparison between analytical (solid line) and CST microwave studio simulated (broken line) results.

Table 3. Properties of different material used in the analysis.

Material	Density (Kg/m^3)	Thermal Conductivity (W/m·K)	Specific Heat (J/Kg·K)	Emissivity	Young's Modulus (Gpa) $\times 10^9$	Thermal expansion (10^{-6}/°C)	Poisson's ratio
Molybdenum	10220	138	251	0.20	324.8	5.1	0.293
Kovar	8360	24.5	649	0.15	14.1	4.81	0.30
Monel	8840	26.04	546	0.06	114	137	0.25
Nickel	8900	76.2	594	0.19	199.5	13.3	0.312
Diamond	3010	1800	5.02	0.03	1050	1.0	0.2
Alumina 96%	3900	28-35	880	0.4	300	8.2	0.21

$\sim$13 GHz and minor shift in frequency. This is because helix is a non-resonant structure, but due to variation of helix pitch, small amount of resonance occurs. The discrepancy in result may be due to analytical programme uses characteristic impedance of helix and CST uses wave impedance.

Thermal and structural analysis of the coupler has been carried out in ANSYS with respect to its thermal management. Due to thermal load in the coupler, temperature distributions at different regions are shown in Figure 3. The boundary conditions used in the simulation are given in Tables 1 and 2, and the properties of different materials used in simulation are given in Table 3. Temperature

Table 4. Thermal and structural parameters of alumina window disc.

Part	**Maximum Temperature (°C)**	**Maximum Displacement (mm)**		**Maximum Stresses (MPa)**
		Radial	**Axial**	
Center Pin	134.35	1.43*e*-004	1.3139*e*-003	0.12673
Tubing	127.61	1.327*e*-004	2.922*e*-003	5.8037
Window Ceramic	115.35	1.2861*e*-003	1.431*e*-003	32.158
Window Cup	92.51	1.2868*e*-003	2.0886*e*-003	1.1678
RF arm	63.08	1.956*e*-003	1.9636*e*-003	11.074

Table 5. Thermal and structural parameters of diamond window disc.

Part	**Maximum Temperature (°C)**	**Maximum Displacement (mm)**		**Maximum Stresses (MPa)**
		Radial	**Axial**	
Center Pin	134.27	1.2073*e*-004	1.6849*e*-003	0.2269
Tubing	120.07	1.9581*e*-004	1.7522*e*-003	8.2961
Window Ceramic	95.007	1.3766*e*-003	7.8334*e*-004	9.9899
Window Cup	94.792	1.4998*e*-003	1.2416*e*-003	1.1514
RF arm	63.84	1.9404*e*-003	1.0876*e*-003	8.5948

distribution and structural properties of the MSCC are tabulated in Table 4. It can be seen from Table 4 that maximum temperature is reached in the center conductor and gradually decreases outward. Heat dissipation from center conductor takes place through ceramic window. MSCC assembly is very delicate and has several brazing joints. Due to non-uniform temperature distribution in the MSCC, expansion of different parts and stress developed at different brazing joints has been studied and presented in Tables 4–5.

Thermal and structural analysis of the coupler with diamond disc has been carried out and results are tabulated in Table 5. It can be seen from Tables 5 that heat dissipation is faster in diamond window disc. Structural deformations and stress developed at different brazing joints are less for diamond window disc, and hence, diamond is a better choice for designing of coupler. However, due to cost effectiveness, alumina disk is an alternative choice for low to medium power applications.

5. CONCLUSION

MSCC is capable of handling high power propagation. However, it needs proper matching of both source and load impedances to avoid multiple reflections which is very tedious and takes several iteration cycles, and commercial software packages take very long time for each iteration cycle. This motivated to develop an analytical model to reduce iteration cycle. The analytical model developed based on reflection approach that is minimization of reflection from quarter-wave transformer through impedance matching. The analytical model agrees closely with CST microwave studio simulated results and takes considerably less iteration time than commercial packages. Moreover, this two-dimensional analytical model is more general and easy to understand and may find potential application in designing coaxial couplers for vacuum devices in the first hand. Thermal and structural analysis of the coupler increases the potential of the analysis as it shows effect of thermal loading on these behaviors. Thermal analysis shows the benefits of CVD diamond over alumina; however, the former is more cost effective.

REFERENCES

1. Kim, H. S., H. S. Uhm, and S. W. Baek, "Thermal and structural analysis on output coupler of helix-TWT," *Proceedings of 30th IEEE International Conference on Plasma Science (ICOPS)*, 174, Jun. 2003.
2. Sinha, A. K., V. V. P. Singh, V. Srivastava, and S. N. Joshi, "On the design of coaxial coupler having multi-section short transformer for compact sized power helix travelling wave tubes," *IEEE Vacuum Electronics Conference*, Monterey, CA, USA, 2000.
3. Baik, C.-W., B. Jia, S.-S. Jung, and G.-S. Park, "Matching of the helix with coaxial coupler," *2000 25th International Conference on Infrared and Millimeter Waves, Conference Digest*, 337–338, Beijing, China, 2000.
4. Alaria, M. K., A. K. Sinha, and V. Srivastava, "Thermal analysis of coaxial coupler for a space helix TWT," *India Journal of Radio & Space Physics*, Vol. 38, 227–232, Aug. 2009.
5. Ghosh, T. K., R. G. Carter, A. J. Challis, K. G. Rushbrook, and D. Bowler, "Optimization of coaxial couplers," *IEEE Transactions on Electron Devices*, Vol. 54, No. 7, 1753–1759, 2007.
6. Ghosh, S., P. K. Jain, and B. N. Basu, "Rigorous tape analysis of inhomogeneously loaded slow-wave structures," *IEEE Trans. on Electron Devices*, Vol. 44, No. 7, 1158–1168, 1997.
7. Gilmour, A. S., *Principles of Traveling Wave Tubes,* Artech House, Boston, 1994.
8. Collin, R. E., *Foundations for Microwave Engineering,* 2nd Edition, McGrew-Hill, Inc., 1992.
9. Kim, H. J., Y. H. Na, J. J. Choi, and J. H. So, "Experimental investigation of a helical traveling-wave tube designed by accurate numerical modeling," *Journal of the Korean Physical Society*, Vol. 50, No. 1, 72–77, 2007.
10. CST Studio Suite 2010 Operating Manual, Licensed 2010, Darmstadt, Germany, 2010.
11. ANSYS Help Guide, Version 10.1, ANSYS Inc.